Search for Dark Particles at Belle

Eunil Won[1] *(on behalf of the Belle Collaboration)*

[1]Korea University, South Korea

DOI: http://dx.doi.org/10.3204/DESY-PROC-2016-03/Won_Eunil

We search for dark photon A' and the dark Higgs boson h' particles that are suggested in number of recently proposed dark sector models. We present our search results in the production of $e^+e^- \to A'h'$ with the decay mod of $h' \to A'A'$. The search was carried out in both inclusive and exclusive modes. We also discuss future prospects of the dark particle search with the Belle II experiment that aims to start in 2018.

1 Introduction

The dark particles were originally considered as a new spin-1 boson for new physics [1] beyond the Standard Model and this proposed the dark sector can be at least a part of dark matter that has not seen yet in hadron collider based searches [2, 3]. The dark boson A' can be produced in a radiative e^+e^- collision via kinetic mixing of a virtual photon with the kinetic mixing parameter ϵ and is illustrated in Fig. 1. This new dark boson requires an extended Higgs sector to break the new $U(1)'$ symmetry and is commonly referred as the dark Higgs h'. In this presentation, we search for the dark boson and the dark Higgs in both exclusive and inclusive modes.

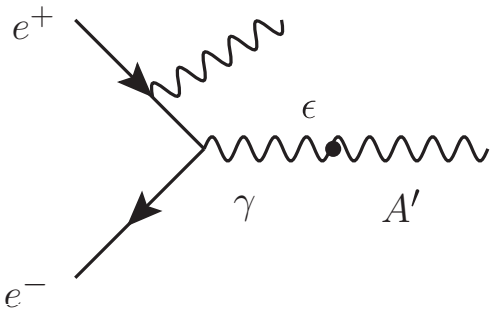

Figure 1: An example Feynman diagram that illustrates production of the dark photon A' in e^+e^- collision.

2 Data Analysis

2.1 Experimental facility and the data set

We use data collected with the Belle detector [4] at the KEKB e^+e collider [5] , amounting to 977 fb^{-1} at center-of-mass energies corresponding to the $\Upsilon(1S)$ to $\Upsilon(5S)$ resonances and in the nearby continuum. We optimize the selection criteria and determine the $e^+e \to A'h'$ signal detection efficiency using a Monte Carlo (MC) simulation where the interaction kinematics and detector response are simulated with the packages MadGraph [6] and GEANT3 [7], respectively. There is no suitable background simulation available, so background samples are taken from data sidebands.

2.2 Main Analysis in Detail

We study the Higgs-strahlung channel, $e^+e^- \to A'h'$. The dark photon A' can decay into lepton pairs, hadrons, or invisible particles while the dark Higgs boson h' can decay into either A', $A'^{(*)}$, leptons pairs, or hadrons, where A'^* is a virtual dark photon [8]. The production

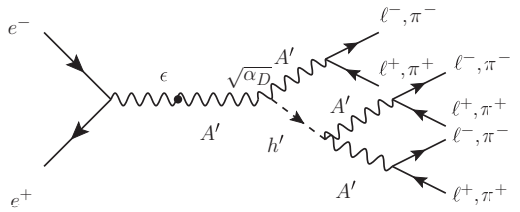

Figure 2: The Feynman diagram that illustrates the Higgs-strahlung channel that we use in this analysis.

and decay modes that we search is indicated in Fig. 2 where α_D is the dark sector coupling constant. In total there are 10 exclusive channels: $3(\ell^+\ell^-)$, $2(\ell^+\ell^-)(\pi^+\pi^-)$, $(\ell^+\ell^-)$ 2 $\pi^+\pi^-)$, and $3(\pi^+\pi^-)$. We also look at 3 inclusive modes for $m_{A'} > 1.1$ GeV/c^2: $2(\ell^+\ell^-)X$ where X is the missing mass from the dark photon candidate.

For the background estimation, we use the same esign events from $e^+e^- \to (\ell^+\ell^+)$ $(\ell^-\ell^-)$ $(\ell^+\ell^-)$, order masses of lepton (or hadron) pairs as $m^1_{\ell\ell} > m^2_{\ell\ell} > m^3_{\ell\ell}$, and plot $m^1_{\ell\ell} - m^3_{\ell\ell}$ vs. $m^1_{\ell\ell}$. Then select the region in invariant mass distribution and predict the background using the same sign events.The figure 3 shows an example invariant mass distribution difference $m^1_{A'_{\rm cand}}$ - $m^2_{A'_{\rm cand}}$ for the $3(\pi^+\pi^-)$ final state. The normalization is from the side band same sign events and the background in the signal region is counted from the same sign events. The background estimation from MC events and real data agree each other and no significant access of signal events is seen in the data at the signal region defined in Fig. 3.

Figure 4 (a) shows the distribution of $m_{A'_{\rm cand}} m_{A'_{\rm cand}}$ as a function of $m_{A'_{\rm cand}}$. Scattered events are largely from inclusive modes or from $3(\pi^+\pi^-)$ states where larger background events are expected. Fig;ure 4 (b) and (c) show the projections on the mass axis of the dark Higgs boson and dark photon, respectively. The of events observed in the signal region, $N_{\rm obs}$, and the number of predicted background events, $N_{\rm bkg}$, are in good agreement. Their differences are quantified by the normalized reduals, shown in Fig. 4 (d) and defined as $(N_{\rm obs} - N_{\rm bkg})$

$\sqrt{\sigma_{\rm obs}^2 + \sigma_{\rm bkg}^2}$, where $\sigma_{\rm obs}$ and $\sigma_{\rm bkg}$ are the standard deviations of the distributions. In all cases, the number of events observed is consistent with the background estimate. For exclusive final states, the background is mostly due to processes with ρ and ω resonance paritlces, such as SM 2γ processes. The discontinuity at 1.1 GeV/c^2 in Fig. 4 (c) is an artifact of the selection criteria.

The upper limit on the $\alpha_D \times \epsilon^2$ are computed based on equations described in Ref [8]. Figure 5 shows the 90 % credibility level (CL) upper limits on $\alpha_D \times \epsilon^2$ for Belle, expected and measured, and for BaBar, for five different mass hypotheses for the dark Higs boson (top row) and dark photon (bottom row) masses.

Note that the inclusion of $3(\pi^+\pi^-)$ final state dramatically improves the limit around the ρ and ω resonances. The dominant source of systematic uncertainties are : the integrated luminosity (1%), branching fractions (4%), track identification (6%), particle identification efficiency (5%), detection efficiency (15%), background estimation (10%), and initial-state radiation (15%). All systematic uncertainties added in quadrature aount to 25%.

2.3 Other Ongoing Analyses

We are also working on a long lived dark photon search where $c\tau$ can be as long as 1-10 cm. Since it is low multiplicity final state (two charged tracks and one photon), the efficiencies are low in general in Belle and one analysis is ongoing. Another analysis is a search for invisible decays when the dark photon decays to a pair of dark matter particles [11]. Since this is a final state with a single photon only, the Belle analysis relies on the photon conversion technique. There is also a study going on based on a new possibility of a dark boson coupling to quarks predominantly, based on Ref. [12].

3 Future Prospects

The KEKB e^+e^- collider and the Belle detector are under major upgrade to the superKEKB collider and the Belle II detector in order to acheive the collection of 50 times more data [13]. The Belle II detector will be in fact a brand new detector except the crystal based electromagnetic calorimeter. A two-layer pixel and silicon strip detectors will function as the new vertex detector, and a newly constructed drift chamber provide precision charged particle tracking as well as 3-dimensional online track trigger. Time of propagation counter based particle identification system for barrel and the proximity focusing aerogel ring image Chrenkov detector for the end are now under construction. New resistive plate counter for the barrel and the sciltillator with the multi-pixel photon counter readout is constructed for the endcap muon and K_L particle detection. The full detector operation is expected in 2018.

This upgrades enables us to be dramatically sensitive to the search for new particles in the dark sector. This is not only due to the increase of the data size by 50 times but also due to much improved the online trigger system. The detailed track and energy cluster information is sent to all the way down to the final global trigger logic unit and this will enable us to prepare dedicated trigger lines for the dark particle searches. From this one expect to explore the kinematic mixing parameter values of just above 10^{-4} in the dark photon mass values of 0.01 to 10 GeV/c^2.

4 Bibliography

References

[1] P. Fayet, "Effects of the Spin-1 Partner of the Goldstino (Gravitino) on Neutral Current Pheomenology," Phys. Lett. B **95**, 285 (1980).

[2] G. Aad *et al.*, [ATLAS Collaboration], "Summary of the ATLAS experiments sensitivity to supersymmetry after LHC Run 1 interpreted in the phenomenological MSSM," J. High Energy Phys. **10**, 134 (2015).

[3] S. Chatrchyan *et al.*, [CMS Collaboration], "Interpretation of searches for supersymmetry with simplified models," Phys. Rev. D **88**, 052016 (2013).

[4] A. Abashian *et al.* [Belle Collaboration], Nucl. Instrum. Methods Phys. Res. Sect. A **479**, 117 (2002); also see detector section in J.Brodzicka et al., Prog. Theor. Exp. Phys. **2012**, 04D001 (2012).

[5] S. Kurokawa and E. Kikutani, Nucl. Instrum. Methods Phys. Res. Sect. A **499**, 1 (2003), and other papers included in this Volume; T. Abe *et al.*, Prog. Theor. Exp. Phys. 2013, 03A001 (2013) and following articles up to 03A011.

[6] J. Alwall P *et al.*, "The automated computation of tree-level and next-to-leading order differential cross sections, and their matching to parton shower simulations", J. High Energy Phys. **07**, 079 (2014).

[7] R. Brun *et al.*, GEANT 3.21, Cern/DD/ee/84-1, (1986).

[8] B. Batell, M. Pospelov, and A. Ritz, "Proving a secluded $U(1)$ at B factories", Phys. Rev. D **79**, 115008 (2009).

[9] I. Jaegle *et al.* [Belle Collaboration], "Search for the dark photon and the dark Higgs boson at Belle", Phys. Rev. Lett. **114**, 211801 (2015).

[10] J. P. Lees *et al.* [BaBar Collaboration], "Search for Low-Mass Dark-Sector Higgs Bosons", Phys. Rev. Lett. **108**, 211801 (2012).

[11] R. Essig, J. Mardon, M. Papucci, T. Volansky, and Y. Zhong, "Constraining light dark matter with low-energy e^+e^- colliders", J. High Energy Phys. **11**, 167 (2013).

[12] S. Tulin, "New weakly coupled forces hidden in low-energy QCD", Phys. Rev. D **89**, 114008 (2014).

[13] B. Wang, [for the Belle Collaboration] "The Belle II Experiment and SuperKEKB Upgrade", `arXiv:511.09434`.

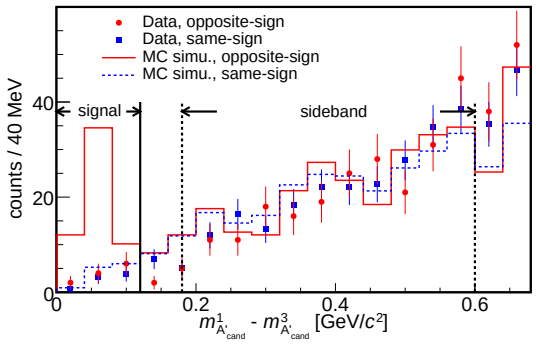

Figure 3: The distribution of $m^1_{A'_{\rm cand}}$ - $m^2_{A'_{\rm cand}}$ for the $3(\pi^+\pi^-)$ final state. The solid and dotted histograms are from opposite-sign and the same-sign MC events. The closed circles (red) and squares (blue) are the data from opposite-sign and the same-sign data events, respectively. The figure is taken from [9].

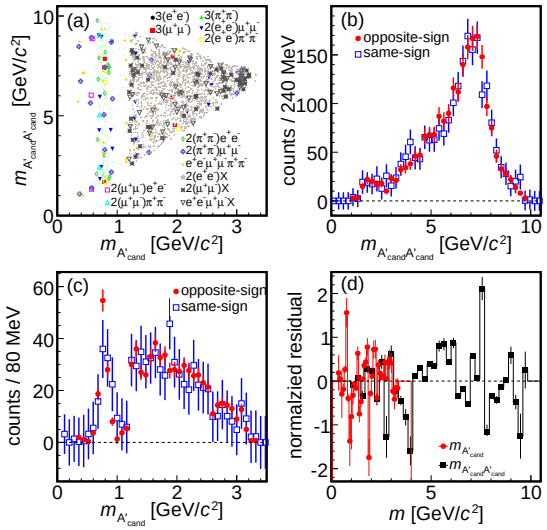

Figure 4: Signal candidates observed versus dark photon candidate mass: $m_{A'_{\rm cand}}$, and dark Higgs boson candidate mass, $m_{A'_{\rm cand}} m_{A'_{\rm cand}}$, for the 13 final states. There are three entries per event. (b) and (c): Projection of signal candidates onto $m_{A'_{\rm cand}} m_{A'_{\rm cand}}$ and $m_{A'_{\rm cand}}$ (red points) with the predicted background (blue squares) from the scaled same-sign distributions for comparison. (d): Normalized reduals between the signal candidate distribution and predicted background, versus dark photon candidate mass (red points) and dark Higgs boson candidate mass (black squares). The figure is taken from [9].

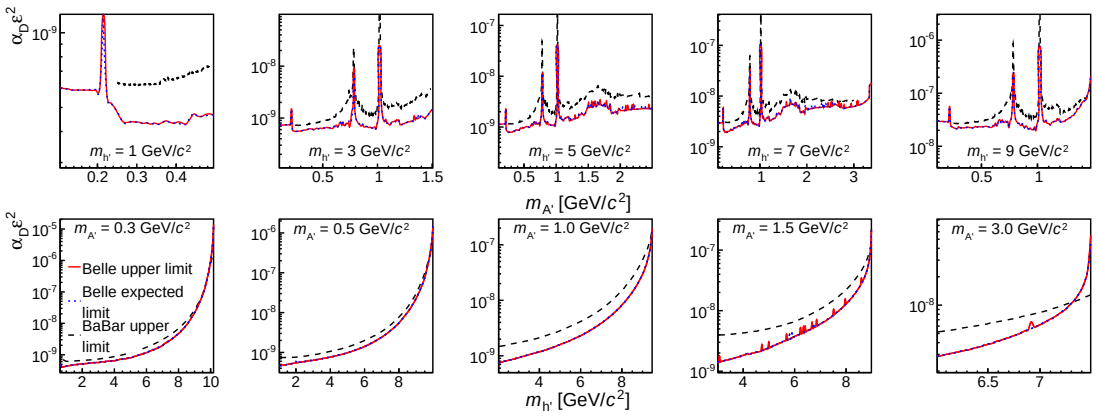

Figure 5: 90 % CL level on the product $\alpha_D \times \epsilon^2$ versus dark photon mass (top row) and dark Higgs boson mass (bottom row) for Belle (solid red curve) and BaBar [10] (dashed black curve). The blue dotted curve, which coincides more or less with the solid red curve, shows the expected Belle limit. The figure is taken from [9].